



Publication Year	2018
Acceptance in OA	2020-10-22T11:49:45Z
Title	DEMNUi: massive neutrinos and the bispectrum of large scale structures
Authors	Ruggeri, Rossana, Castorina, Emanuele, CARBONE, Carmelita, SEFUSATTI, Emiliano
Publisher's version (DOI)	10.1088/1475-7516/2018/03/003
Handle	http://hdl.handle.net/20.500.12386/27918
Journal	JOURNAL OF COSMOLOGY AND ASTROPARTICLE PHYSICS
Volume	2018

DEMNUi: Massive neutrinos and the bispectrum of large scale structures

Rossana Ruggeri,^a Emanuele Castorina,^b Carmelita Carbone,^{c,d,e}
Emiliano Sefusatti^{f,g}

^aInstitute of Cosmology & Gravitation, University of Portsmouth, Dennis Sciana Building, Portsmouth PO1 3FX — UK

^bBerkeley Center for Cosmological Physics, University of California, Berkeley, CA 94720, USA, and Lawrence Berkeley National Laboratory, 1 Cyclotron Road, Berkeley, CA 93720, USA

^cUniversità degli Studi di Milano - Dipartimento di Fisica, via Celoria 16, I-20133 Milano (MI), Italy

^dINAF - Osservatorio Astronomico di Brera, via Brera 28, I-20121 Milano (MI) – Italy

^eINFN - Sezione di Milano, via Celoria 16, I-20133, Milano (MI) – Italy

^fINAF - Osservatorio Astronomico di Trieste, via Tiepolo 11, I-34143 Trieste – Italy

^gINFN - Sezione di Trieste, Via Valerio 2, I-34127 Trieste – Italy

E-mail: rossana.ruggeri@port.ac.uk, ecastorina@berkeley.edu,
carmelita.carbone@unimi.it, emiliano.sefusatti@brera.inaf.it

Abstract. The main effect of massive neutrinos on the large-scale structure consists in a few percent suppression of matter perturbations on all scales below their free-streaming scale. Such effect is of particular importance as it allows to constraint the value of the sum of neutrino masses from measurements of the galaxy power spectrum. In this work, we present the first measurements of the next higher-order correlation function, the bispectrum, from N-body simulations that include massive neutrinos as particles. This is the simplest statistics characterising the non-Gaussian properties of the matter and dark matter halos distributions. We investigate, in the first place, the suppression due to massive neutrinos on the matter bispectrum, comparing our measurements with the simplest perturbation theory predictions, finding the approximation of neutrinos contributing at quadratic order in perturbation theory to provide a good fit to the measurements in the simulations. On the other hand, as expected, a linear approximation for neutrino perturbations would lead to $\mathcal{O}(f_\nu)$ errors on the total matter bispectrum at large scales. We then attempt an extension of previous results on the universality of linear halo bias in neutrino cosmologies, to non-linear and non-local corrections finding consistent results with the power spectrum analysis.

Keywords: Cosmology, Large Scale Structure of the Universe, Galaxy clustering; Neutrino physics

Contents

1	Introduction	1
2	Cosmological perturbations in the presence of massive neutrinos	2
2.1	Linear evolution	2
2.2	Nonlinear evolution	3
3	The DEMNUni simulations suite	5
4	The matter bispectrum	6
5	The halo bispectrum	12
5.1	Bias modeling	12
5.2	Fitting procedure	13
5.3	The universality of the halo bias at quadratic order	14
6	Conclusions	16

1 Introduction

Despite the constant improvement in the quality of observations over the last decade, the Standard, Λ CDM, Cosmological model, still provides a good fit to several cosmological observables [1–3]. It is therefore clear that the analysis of future galaxy survey data [4–6] will require accurate predictions, at the percent level or better, since any departure from the standard scenario will likely be relatively small [7–18].

In this context, it has become necessary to properly account for the effects of neutrino masses on cosmological observables. Massive neutrinos represent a small but non negligible fraction of the matter density, characterised by a significant thermal velocity distribution even when non-relativistic, and we should account for the different evolution of their perturbations with respect to the cold dark matter component. Their overall effect consists in a damping of matter perturbations on all scales below their free-streaming scale: a several percent reduction on the *total* matter power spectrum, [19, 20]. This happens precisely on the range of scales probed by current galaxy redshift surveys (tens to hundreds of Megaparsecs). In fact, cosmological observations are able to provide an upper limit to the (sum of) neutrino masses [2, 21–25] and, in the long run, possibly bridge the gap with the lower limit given by neutrino oscillation experiments [4, 5]. In other terms, neutrino masses are not simply a nuisance in the possible detection of dark energy or new physics effects, but represent an important test for the Standard Model of particles physics and its extensions.

Several studies had appeared, over the last few years, on massive neutrinos effects on the matter power spectrum nonlinear evolution and redshift-space distortions in the context of perturbation theory [26–38], on baryonic acoustic oscillations [39, 40], on the halo mass function [33, 41–44], halo bias [33, 42, 45–48] and cosmic voids [49]. Novel probes of massive neutrinos have also been recently proposed [50, 51].

Focusing on the theoretical description of matter perturbations, predictions for the nonlinear matter power spectrum have been first studied in [26] and [27]. The model proposed for the *total* matter power spectrum approximates neutrino perturbations with their linear prediction (obtained from a Boltzmann code, and therefore acting as a source for cold and baryonic matter), limiting nonlinear corrections only to the *cold* dark matter component. The limits of this approximation are carefully studied in both works, estimating systematic errors due to the linear neutrino assumption to be at the sub-percent level. Indeed, comparisons with particle-based N-body simulations show the discrepancies between numerical results and predictions based on Perturbation Theory (PT) in the massive neutrino case to be consistent with the typical accuracy of the standard PT approach in

Λ CDM models [33]. The validity of the linear neutrino approximation is further explored in [30, 52] where the authors highlight how the violation of momentum conservation inherent in the scheme might have significant effects in the nonlinear corrections beyond the 1-loop level. They propose an hybrid model combining the full Boltzmann treatment at high redshift and the two-fluid approximation at later times as a starting point for studying the nonlinear evolution. In this approximation, both cold dark matter (including baryons) and neutrinos are described as fluids, the second characterised by a (time-dependent) effective speed of sound, estimated from the neutrino velocity dispersion [53]. Explicit predictions for the matter bispectrum have been presented, so far, in [34] and [37]. Ref. [34] presents a test of the two-fluid and the linear neutrinos approximations, against the exact treatment via the collisionless Boltzmann equation, using the bispectrum as a specific measure of their validity at the level of higher-order corrections. They show how both approximations fail to provide a 1% accuracy on the total matter bispectrum. In particular, as we will discuss, the linear neutrinos approximation does not correctly reproduce the large scale matter bispectrum for large neutrino masses, while in the limit of a small neutrino density fraction, f_ν , becomes significantly more accurate. The same limit is also explored in the alternative formulation of [37], where a perturbative expansion around $f_\nu = 0$ is considered.

In this work we present, for the first time, measurements of the matter and halo bispectrum in N-body simulations that include a massive neutrino component as particles. In the case of the two matter components, neutrinos and cold dark matter/baryons, we provide a first comparison with theoretical predictions assuming neutrinos perturbations at next-to-leading order in PT. In addition, we attempt an extension of the results of [42] on the “universality” of linear halo bias to the nonlinear level, including as well non-local corrections [54, 55]. In fact, the bispectrum, as a direct result of nonlinear evolution, provides a valuable test of nonlinear effects (due to both gravitational instability and bias) in these, by now, standard cosmological models. Moreover, the galaxy bispectrum, is the lowest-order statistic encoding and quantifying the non-Gaussian properties of the galaxy distribution [56]. Several groups have measured three-point statistics in recent data [57, 58], showing that the adding this information to the standard power spectrum analysis yield to better constraints on the cosmological parameters.

The paper is organized as follow. In Sec. 2 we briefly review basic results on massive neutrinos perturbations. In Sec. 4 we show our measurements of the bispectrum for the various matter components and compare them with theoretical predictions from perturbation theory, while in Sec. 5 we show the halo bispectrum measurements and derive the corresponding halo bias functions. In Sec. 6 we conclude summarising the results obtained.

2 Cosmological perturbations in the presence of massive neutrinos

2.1 Linear evolution

In the early Universe neutrinos are kept in equilibrium with baryons and photons via weak interactions, eventually decoupling at a temperature of about $T_{\text{dec}} \sim 9 \times 10^9$ K, when their interaction rate becomes comparable to rate of cosmological expansion. After decoupling, neutrinos free-stream with large thermal velocities described by a Fermi-Dirac distribution. As the Universe expands neutrinos slow down, becoming non relativistic at a typical redshift of

$$1 + z_{nr} \simeq 1980 \frac{m_{\nu,i}}{1 \text{ eV}}, \quad (2.1)$$

where $m_{\nu,i}$ represents the neutrino mass eigenstate i in electronvolt. As non-relativistic particles, while contributing to the total matter density the fraction

$$f_\nu \equiv \frac{\Omega_\nu}{\Omega_m} = \frac{1}{\Omega_{m,0} h^2} \frac{\sum_i m_{\nu,i}}{93.14 \text{ eV}}, \quad (2.2)$$

they still travel much longer distances, of the order of tens of Megaparsecs, compared to standard cold dark matter (CDM) particles. We define a free-streaming length $\lambda_{\text{fs}} \propto v_{th}/H(t)$, with v_{th} being the

characteristic thermal velocity of neutrino particles. Below this scale we expect a suppression of the neutrino density fluctuations with respect to CDM ones. On scales $\lambda \gg \lambda_{\text{fs}}$ we expect neutrinos to behave as CDM. In Fourier-space, the wavenumber corresponding to λ_{fs} can be written as

$$k_{\text{fs}} \simeq \frac{0.908}{\sqrt{1+z}} \sqrt{\Omega_{m,0}} \frac{m_{\nu,i}}{1 \text{ eV}} h \text{ Mpc}^{-1}. \quad (2.3)$$

For simplicity we denote with the subscript “ c ” quantities related to the CDM *and* baryonic matter components as no distinction will be made between the two. We refer to such component generically as “cold” matter, as opposed to the neutrinos contribution. Total matter perturbations are therefore given by the weighted sum

$$\delta_m = (1 - f_\nu)\delta_c + f_\nu\delta_\nu. \quad (2.4)$$

with δ_ν denoting neutrinos perturbations.

On scales smaller than λ_{fs} neutrinos do not provide support to the Newtonian gravitational potential, and we expect the growth of cold matter perturbations to be different with respect to a standard cosmology. It is possible to show [59] that, in linear theory, for $k \gg k_{\text{fs}}$, assuming a constant Ω_m and a constant amplitude for primordial fluctuations, the ratio of the cold matter power spectra in a cosmology with $f_\nu \neq 0$ to the massless neutrino case is given by

$$\frac{P_{cc}^{f_\nu \neq 0}(k)}{P_{cc}^{f_\nu = 0}(k)} \stackrel{k \gg k_{\text{fs}}}{\simeq} 1 - 6 f_\nu. \quad (2.5)$$

The total matter power spectrum, from eq. 2.4, can be written as

$$P_{mm}(k) = (1 - f_\nu)^2 P_{cc}(k) + 2f_\nu(1 - f_\nu)P_{\nu c}(k) + f_\nu^2 P_{\nu\nu}(k), \quad (2.6)$$

with $P_{\nu c}(k)$ denoting the cold matter-neutrinos cross-power spectrum. Neglecting neutrino perturbations at small scales we obtain the well-known limit [59]

$$\frac{P_{mm}^{f_\nu \neq 0}(k)}{P_{mm}^{f_\nu = 0}(k)} \stackrel{k \gg k_{\text{fs}}}{\simeq} 1 - 8 f_\nu. \quad (2.7)$$

2.2 Nonlinear evolution

Numerical simulations [60–65] have shown that the suppression expected in linear theory according to eq. 2.5 and 2.7 is enhanced at the nonlinear level, as expected from predictions in perturbation theory [26, 27], with important consequences for the constraints on neutrino masses [13, 26].

On the other hand, a direct consequence of the nonlinear evolution of matter fluctuations is given by the emergence of non-Gaussianity, quantified, in the first place by a non-vanishing matter bispectrum. Denoting the cold matter fraction as $f_c \equiv 1 - f_\nu$, the analogue of eq. 2.6 for the total matter bispectrum is given by

$$B_{mmm}(k_1, k_2, k_3) = f_c^3 B_{ccc}(k_1, k_2, k_3) + f_c^2 f_\nu B_{cc\nu}^{(s)}(k_1, k_2, k_3) + f_c f_\nu^2 B_{\nu\nu c}^{(s)}(k_1, k_2, k_3) + f_\nu^3 B_{\nu\nu\nu}(k_1, k_2, k_3) \quad (2.8)$$

where we introduced the symmetrized versions of the cross cold-cold-neutrino bispectrum $B_{cc\nu}^{(s)}$ and neutrino-neutrino-cold bispectrum $B_{\nu\nu c}^{(s)}$ defined, respectively, as

$$\delta_D(\mathbf{k}_{123}) B_{cc\nu}^{(s)}(k_1, k_2, k_3) \equiv [\langle \delta_c(\mathbf{k}_1)\delta_c(\mathbf{k}_2)\delta_\nu(\mathbf{k}_3) \rangle + \langle \delta_c(\mathbf{k}_3)\delta_c(\mathbf{k}_1)\delta_\nu(\mathbf{k}_2) \rangle + \langle \delta_c(\mathbf{k}_2)\delta_c(\mathbf{k}_3)\delta_\nu(\mathbf{k}_1) \rangle] \quad (2.9)$$

and

$$\delta_D(\mathbf{k}_{123}) B_{\nu\nu c}^{(s)}(k_1, k_2, k_3) \equiv [\langle \delta_c(\mathbf{k}_1)\delta_\nu(\mathbf{k}_2)\delta_\nu(\mathbf{k}_3) \rangle + \langle \delta_c(\mathbf{k}_3)\delta_\nu(\mathbf{k}_1)\delta_\nu(\mathbf{k}_2) \rangle + \langle \delta_c(\mathbf{k}_2)\delta_\nu(\mathbf{k}_3)\delta_\nu(\mathbf{k}_1) \rangle]. \quad (2.10)$$

where we made use of the notation $k_{ij} \equiv \mathbf{k}_i + \mathbf{k}_j$ for vectors sums.

Although neutrinos cluster very weakly below the free streaming scale, on larger scales they behave like CDM. This means that assuming *linear* neutrino perturbation on *any* scale results in a lack of power on the large-scale bispectrum, which is the outcome of the nonlinear evolution of all matter components. As a consequence, numerical simulations treating neutrinos only at the linear level on the grid (or not having neutrino fluctuations at all) will predict the wrong bispectrum as well as any other higher-order correlation function. On the other hand the two fluids behave similarly only in the very low- k regime, and therefore we expect next -to-leading order, *i.e.* quadratic, correction to capture most of the neutrino contributions to the bispectrum terms in the above equations. In analogy with the work in [26, 33] for the matter power spectrum in cosmologies with massive neutrinos we assume neutrinos to contribute only at tree-level in the PT calculation, whereas we compute CDM density perturbations up to the 1-loop level. The analysis in [33] showed that this simple approach reproduces the measurements of the power spectrum in simulations to 1% accuracy. The goal of this section is to test on simulations whether the same assumptions hold true for the bispectrum, within the limits of the precision of our measurements.

At tree-level in PT both the cold matter and the neutrino perturbations in eq. 2.10 contribute to the neutrino-neutrino-cold matter component $B_{\nu\nu c}^{(s)}$, such that

$$B_{\nu\nu c}^{(s),tree}(k_1, k_2, k_3) = B_{\nu\nu c,112}^{(s)}(k_1, k_2, k_3) + B_{\nu\nu c,121}^{(s)}(k_1, k_2, k_3) + B_{\nu\nu c,211}^{(s)}(k_1, k_2, k_3), \quad (2.11)$$

where the subscripts “112” indicate the order of the perturbations δ_ν , δ_ν and δ_c , respectively. It is easy to see that

$$B_{\nu\nu c,211}^{(s)}(k_1, k_2, k_3) = 2 F_2(\mathbf{k}_1, \mathbf{k}_2) P_{\nu c}^L(k_1) P_{\nu\nu}^L(k_2) + 2 \text{ perm} \quad (2.12)$$

$$B_{\nu\nu c,112}^{(s)}(k_1, k_2, k_3) = 2 F_2(\mathbf{k}_1, \mathbf{k}_2) P_{\nu c}^L(k_1) P_{\nu c}^L(k_2) + 2 \text{ perm} \quad (2.13)$$

and $B_{\nu\nu c,121}^{(s)} = B_{\nu\nu c,211}^{(s)}$ (we are assuming the ordering of the subscript to correspond to the perturbations δ_c , δ_c and δ_ν in this order). Setting neutrino perturbations to their linear value on *all scales* leads to $B_{\nu\nu c,121}^{(s)} = B_{\nu\nu c,211}^{(s)} = 0$, resulting, in turn, in a $\mathcal{O}(1)$ bias in $B_{\nu\nu c}$ at scales $k < k_{\text{fs}}$. At the one-loop level, the only contribution is coming from the fourth-order correction to δ_c so that we only have

$$B_{\nu\nu c,114}^{(s)}(k_1, k_2, k_3) = 4 P_{\nu c}^L(k_1) P_{\nu c}^L(k_2) \int d^3q F_4(\mathbf{q}, -\mathbf{q}, \mathbf{k}_1, \mathbf{k}_2) P_{cc}^L + 2 \text{ perm.} \quad (2.14)$$

The full prediction up to one-loop would then be given by

$$B_{\nu\nu c}^{(s)} \simeq B_{\nu\nu c}^{(s),tree} + B_{\nu\nu c,114}^{(s)}. \quad (2.15)$$

For the cold-cold-neutrino component $B_{cc\nu}^{(s)}$ the tree-level expression is the same of eq. 2.12 with the replacement $\nu \leftrightarrow c$ in all the terms. At one-loop we have now three types of contributions,

$$B_{cc\nu,411}^{(s)} = B_{cc\nu,141}^{(s)} = 4 [P_{\nu c}^L(k_1) P_{cc}^L(k_2) + P_{\nu c}^L(k_2) P_{cc}^L(k_1)] \\ \times \int d^3q F_4(\mathbf{q}, -\mathbf{q}, \mathbf{k}_1, \mathbf{k}_2) P_{cc}^L(q) + 2 \text{ perm.}, \quad (2.16)$$

$$B_{cc\nu,321}^{(s)} = 6 P_{\nu c}^L(k_1) \int d^3q F_3(\mathbf{k}_1, \mathbf{k}_2 - \mathbf{q}, \mathbf{q}) F_2(\mathbf{k}_2 - \mathbf{q}, \mathbf{q}) P_{cc}^L(|\mathbf{k}_2 - \mathbf{q}|) P_{cc}^L(q) \\ + 2 \text{ perm.} \quad (2.17)$$

with the additional $B_{cc\nu,231}^{(s)}$ term obtained by exchanging \mathbf{k}_1 with \mathbf{k}_2 , and

$$B_{cc\nu,312}^{(s)} = 6 P_{cc}^L(k_1) \int d^3q F_3(\mathbf{k}_1, \mathbf{k}_2 - \mathbf{q}, \mathbf{q}) F_2(\mathbf{k}_2 - \mathbf{q}, \mathbf{q}) P_{c\nu}^L(|\mathbf{k}_2 - \mathbf{q}|) P_{cc}^L(q) + 2 \text{ perm.} \quad (2.18)$$

with an analogous $B_{cc\nu,132}^{(s)}$. Up to one-loop correction we have then

$$B_{cc\nu}^{(s)} \simeq B_{cc\nu}^{(s),tree} + 2B_{cc\nu,411}^{(s)} + B_{cc\nu,321}^{(s)} + B_{cc\nu,231}^{(s)} + B_{cc\nu,312}^{(s)} + B_{cc\nu,132}^{(s)}. \quad (2.19)$$

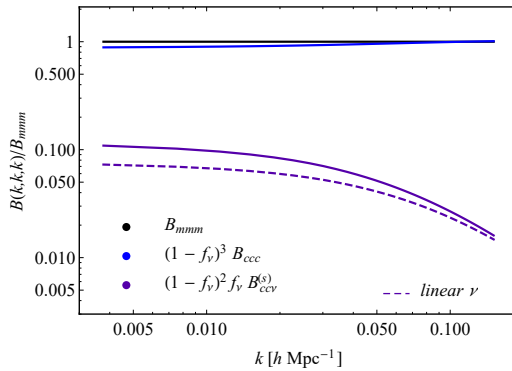


Figure 1. Relative contributions to the equilateral configurations of the total matter bispectrum from the different terms in eq. (2.8) up to $\mathcal{O}(f_\nu)$ for $m_\nu = 0.53$ eV at $z = 0$. The dashed line shows the assumption neutrinos are linear on all scales.

The B_{ccc} is then given by the usual PT expressions in terms of the cold matter linear power spectrum P_{cc}^L [66]. We notice right away that one-loop corrections to the mixed contributions $B_{\nu\nu c}^{(s)}$ and $B_{cc\nu}^{(s)}$, as we will see in section 4, are essentially irrelevant. More important, instead, are the implications of the linear neutrinos approximation on the tree-level prediction, since the relevant short-comings will take place at large scales. We can also anticipate that assuming linear neutrino perturbations will result in an error of order f_ν on scales larger than the free-streaming scale, which could exceed the % level for realistic value of neutrino masses. This is shown in Fig. (1) for $m_\nu = 0.53$ eV at $z = 0$, where we plot, within tree-level PT, the relative contribution of terms up to $\mathcal{O}(f_\nu)$ to the total matter bispectrum of equilateral configurations. The assumption of linear neutrinos on all scales indeed yields an inconsistent result at low k , $B_{cc\nu}$ is underestimated by more than a factor of 2, with biases of several %s on B_{mmm} .

3 The DEMNUni simulations suite

We make use of the ‘‘Dark Energy and Massive Neutrino Universe’’ (DEMNUi) suite of N-body simulations [67], representing one of the best set of simulations of massive neutrino cosmologies both in terms of mass resolution and volume. A complete description can be found also in [33], here we briefly summarize the main details.

All the simulations assume a baseline cosmology according to the *Planck* results [68], namely a flat Λ CDM model with $h = 0.67$ as Hubble parameter, $n_s = 0.96$ as primordial spectral index, and $A_s = 2.1265 \times 10^{-9}$ for the amplitude of initial scalar perturbations. This implies that simulations with massive neutrinos have lower value of σ_8 with respect to the Λ CDM case. The total matter energy density and the baryonic energy density are set to $\Omega_m = 0.32$ and $\Omega_b = 0.05$ for all cosmologies, while the relative energy densities of cold dark matter, Ω_c (and neutrinos, Ω_ν) vary for each model as $\Omega_c = 0.27, 0.2659, 0.2628$ and 0.2573 , for $m_\nu = 0, 0.17, 0.3$ and 0.53 eV, respectively.

The DEMNUi simulations have been performed using the tree particle mesh-smoothed particle hydrodynamics (TreePM-SPH) code GADGET-3 [69], specifically modified by [61] to account for the presence of massive neutrinos. They are characterised by a softening length $\varepsilon = 20 h^{-1}$ kpc, start at $z_{in} = 99$, and have being performed in a cubic box of side $L = 2000 h^{-1}$ Mpc, containing $N_p = 2048^3$ CDM particles, and an equal number of neutrino particles when $m_\nu \neq 0$. These features make the DEMNUi set suitable for the analysis of different cosmological probes, from galaxy-clustering, to weak-lensing, to CMB secondary anisotropies.

Halos and sub-halo catalogs have been produced for each of the 62 simulation particle snapshots, via the friends-of-friends (FoF) and SUBFIND algorithms included in GADGET-3 [70, 71]. The linking length was set to be 1/5 of the mean inter-particle distance [72] and the minimum number of particles

to identify a parent halo was set to 32, thus fixing the minimum halo mass to $M_{\text{FoF}} \simeq 2.5 \times 10^{12} h^{-1} M_{\odot}$. In this work we consider three lower threshold for the halo mass, $M > 10^{13} h^{-1} M_{\odot}$, $M > 3 \times 10^{13} h^{-1} M_{\odot}$ and $M > 10^{14} h^{-1} M_{\odot}$ and three values for the snapshot redshift, $z = 0$, $z = 0.5$, $z = 1$.

4 The matter bispectrum

We measure the total matter bispectrum B_{mmm} along with all its individual components B_{ccc} , $B_{cc\nu}^{(s)}$, $B_{\nu\nu c}^{(s)}$ and $B_{\nu\nu\nu}$ as defined by eq. (2.8). For all components we consider all triangular configurations defined by discrete wavenumbers multiples of $\Delta k = 3k_f$ with $k_f \equiv 2\pi/L$ being the fundamental frequency of the box, up to a maximum value of $0.38 h \text{ Mpc}^{-1}$. The estimator of the bispectrum is given by

$$\hat{B}(k_1, k_2, k_3) \equiv \frac{k_f^3}{V_B(k_1, k_2, k_3)} \int_{k_1} d^3 q_1 \int_{k_2} d^3 q_2 \int_{k_3} d^3 q_3 \delta_D(\mathbf{q}_{123}) \delta_{\mathbf{q}_1} \delta_{\mathbf{q}_2} \delta_{\mathbf{q}_3} \quad (4.1)$$

where the integrations are taken on shells of size Δk centered on k_i and where

$$V_B(k_1, k_2, k_3) \equiv \int_{k_1} d^3 q_1 \int_{k_2} d^3 q_2 \int_{k_3} d^3 q_3 \delta_D(\mathbf{q}_{123}) \simeq 8\pi^2 k_1 k_2 k_3 \Delta k^3 \quad (4.2)$$

is a normalisation factor counting the number of fundamental triangles in a given triangle bin. Its implementation is based on the algorithm described in [73] and taking advantage of the aliasing reduction technique of [74]. As only one realisation for each cosmology is available, all error bars shown correspond to the Gaussian prediction given, for a generic bispectrum, by [75],

$$\Delta B^2(k_1, k_2, k_3) \simeq s_B \frac{k_f^3}{V_B} P(k_1) P(k_2) P(k_3), \quad (4.3)$$

with $s_B = 6, 2, 1$ for equilateral, isosceles and scalene triangles respectively.

Figure 2 shows the measurements at $z = 0$ of all configurations for all components, *rescaled* by the proper factors as a function of the neutrino fraction, according to eq. (2.8), in order to assess directly the relative contribution to the total matter bispectrum. The bottom half of each panel shows the ratio of each component to the total B_{mmm} . Triangles are ordered with increasing k_1 and assuming $k_1 \geq k_2 \geq k_3$ so that all configurations shown correspond to large-scales with $k_1 \leq 0.1 h \text{ Mpc}^{-1}$. Data points from N-body simulations are compared to tree-level predictions in PT. Theoretical predictions are computed for “effective” values of the wavenumbers defined, for a given configuration of sides k_1 , k_2 and k_3 by

$$\tilde{k}_{1,23} \equiv \frac{1}{V_B} \int_{k_1} d^3 q_1 \int_{k_2} d^3 q_2 \int_{k_3} d^3 q_3 \delta_D(\mathbf{q}_{123}), \quad (4.4)$$

and similarly for the other two values. Differences with respect to evaluations at the center of each k -bin are marginally relevant only for the largest scales.

The first, rather obvious, observation is that the only relevant, *i.e.* above 1% level, contribution to the total matter bispectrum B_{mmm} , in addition to the cold matter bispectrum B_{ccc} , is given by the cross-bispectrum $B_{cc\nu}^{(s)}$ which is of $\mathcal{O}(f_\nu)$. Therefore a proper theoretical description of the matter bispectrum in massive neutrinos cosmologies should focus on both these two components. Here we show a first comparison with tree-level PT, providing rather accurate predictions to the cold matter component B_{ccc} over the scales shown in the figure. Predictions for the $B_{cc\nu}^{(s)}$ and $B_{\nu\nu c}^{(s)}$ are very well described by the assumption neutrinos contribute only at tree-level in PT.

As we consider smaller scales, in the quasi-linear regime, the tree-level approximation becomes more accurate for the cross-bispectra of cold matter and neutrinos because of small-scale suppression of neutrino perturbations. On the other hand, we expect further nonlinear (one-loop) corrections to become important only for the cold matter contribution B_{ccc} . This is the natural extension to higher-order correlation functions of previous results for the total matter power spectrum, where linear theory was sufficiently accurate to describe the neutrinos and cross neutrino-cold matter components $P_{\nu\nu}$ and $P_{c\nu}$, respectively [26, 30, 33].

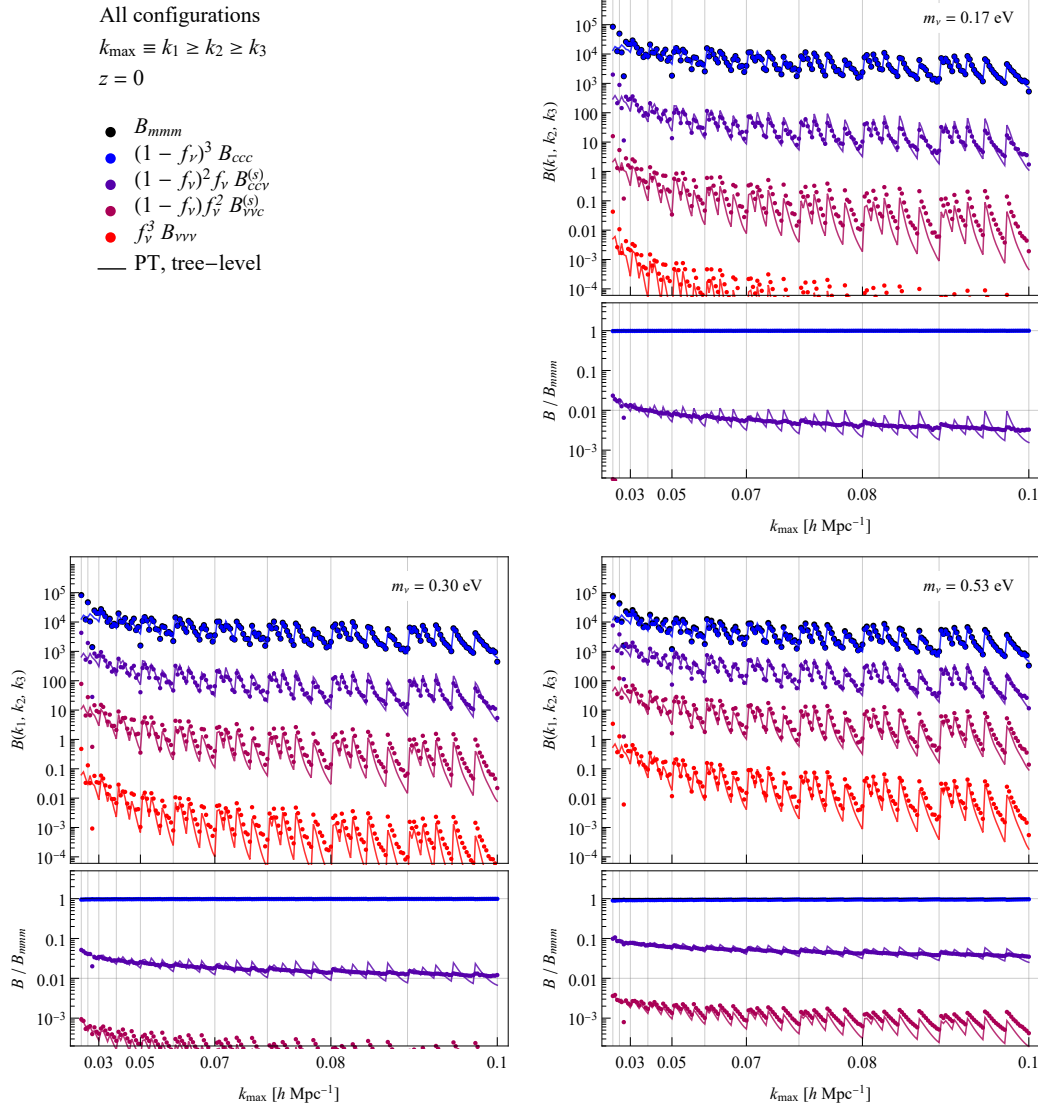


Figure 2. Measurements of all the components of the total matter bispectrum $B_{mmm}(k_1, k_2, k_3)$ at $z = 0$, properly weighted, compared with the tree-level prediction in PT. All triangular configurations are re ordered with increasing k_1 and assuming $k_1 \geq k_2 \geq k_3$. In each panel, the bottom-half shows the relative contribution of each component to B_{mmm} (only the relevant ones, contributing above the 0.1% level are shown). Vertical lines correspond to equilateral configurations.

Figure 3 shows the measurements of the cold matter bispectrum, B_{ccc} , at $z = 0.5$ (left panel) and $z = 1$ (right panel), for equilateral triangles (left panel). We compare with analytical predictions at tree (dashed) and 1-loop (continuous) level in PT [66, 76]. Different colors indicate different value of the sum of neutrino masses, $m_\nu = 0, 0.3, 0.53$ eV (black, red and green respectively).

The analytic curves have been obtained according to the prescription as in [33]; we consider the perturbative kernels in cosmology with massive neutrinos to have the same form as in Λ CDM cosmology and we assume all the effects induced by neutrinos encoded in the linear power spectrum. Our assumptions are justified by previous studies [33, 77] which showed this approximation to work better than a % on the power spectrum analysis. Middle panels show the ratio between the data for the three different cosmologies (Λ CDM and $m_\nu = 0.53$ eV) with respect to their 1-loop predictions (black

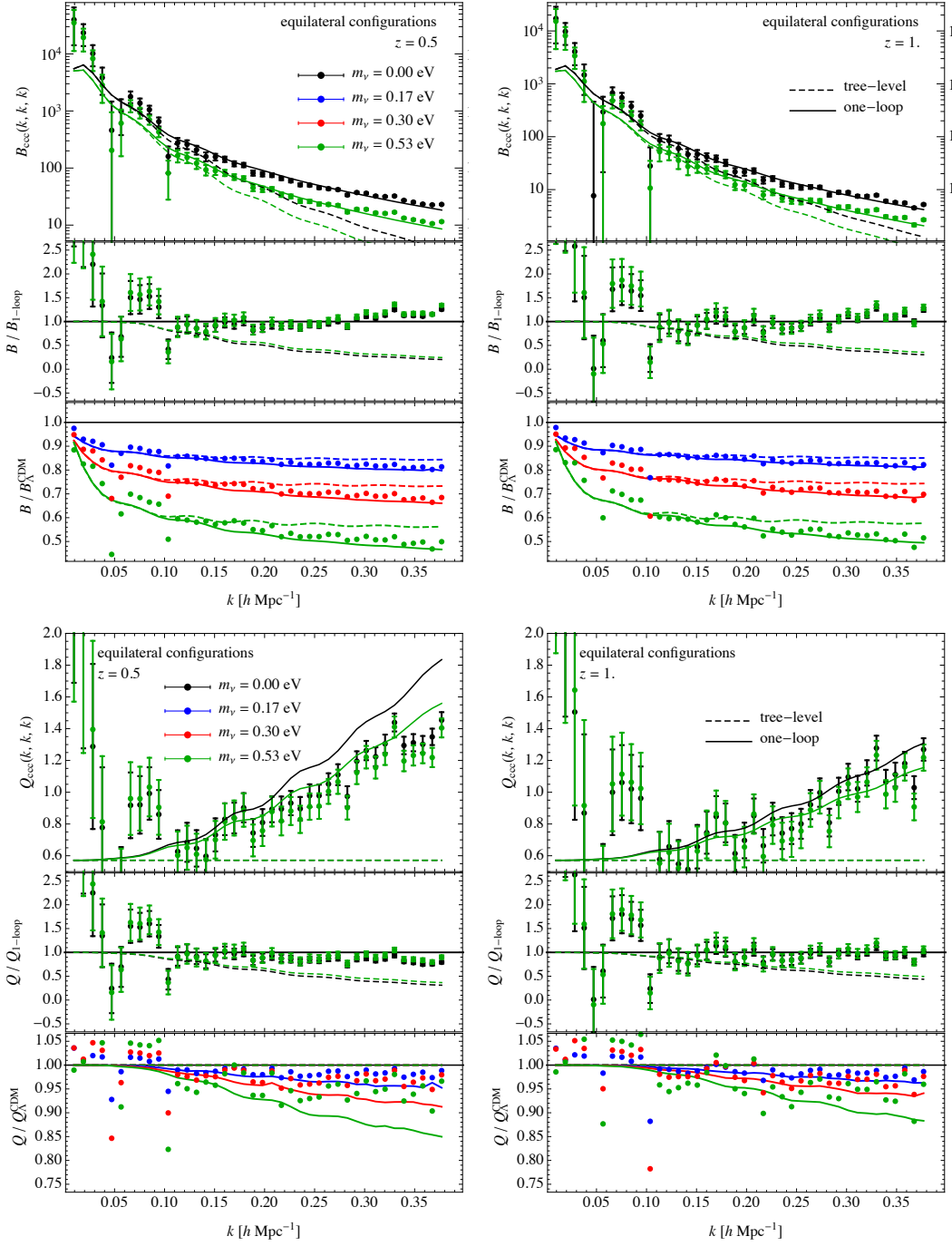


Figure 3. Top panels: equilateral configurations of the cold matter bispectrum, $B_{ccc}(k, k, k)$, compared with tree-level (dashed curves) and one-loop (continuous curves) predictions in PT. Bottom panels: same comparison for the *reduced* cold matter bispectrum $Q_{ccc}(k, k, k)$. Left panels show the results at $z = 0.5$, right panels at $z = 1$. In addition to the measurements of B or Q , we plot the residuals with respect to the one-loop predictions (middle panel) and the ratio between the $m_\nu \neq 0$ cosmologies to the corresponding massless neutrino case (bottom panel).

and green points); we also plot the ratio between tree-level and 1-loop prediction with dashed lines. The approximation of neglecting the effects of massive neutrinos on the 1-loop CDM bispectrum other than the different linear theory $P_{cc}(k)$, provides the same level of agreement we find in the Λ CDM case. In the bottom panels we present the ratio between the bispectrum measured for $m_\nu \neq 0$ with respect to the Λ CDM measurement; continuous and dashed lines denote instead the same ratio as predicted at the 1-loop and tree-level in PT. The comparison with the power spectrum analysis reveals, as expected, that equilateral configurations are roughly two times more sensitive than the power spectrum to massive neutrinos. We also notice that the suppression of CDM bispectrum with respect to the standard case does not evolve significantly with redshift, in agreement with well known results at the two-point function level. As expected [78, 79] one-loop predictions in standard PT tend to overestimate the measurements in equilateral configurations at low redshift. We find a good agreement up to $k = 0.3 h \text{Mpc}^{-1}$ at $z = 0.5$, but it should be kept in mind that the precision of our measurement is roughly 10% at these scales.

A better agreement with measurements can clearly be found in the context of the Effective Field Theory of the Large-Scale Structure [80], see [81] for its application to the matter bispectrum. We limit ourselves to compare the accuracy of standard PT predictions in massive neutrino cosmology with known results for the Λ CDM case.

More generally, the suppression of the amplitude of the bispectrum in cosmology with massive neutrinos compared to a standard cosmological model is a function of the triangle shape. For instance it is easy to see that squeezed triangle configurations, $B_{mmm}(q, k, k)$ with $q \ll k$ are less affected by massive neutrinos. The physical interpretation of this is simple: for significantly large scales, q , the neutrinos behaves like CDM and therefore the relative suppression with respect to the Λ CDM case is reduced compared to other triangular configurations. At a scale where $q \ll k_{fs}$ then $\delta_\nu(q) \simeq \delta_c(q)$ and one has $B_{\nu cc}(q, k, k) \simeq B_{ccc}(q, k, k)$ on all scales, even below free-streaming. While our perturbation theory calculations provide a reasonable fit to the measurements in the N-body, our analysis is in disagreement with the prediction of [37] who have analytically found that squeezed configurations show the largest neutrinos-induced suppression. Squeezed configurations are shown in Figure 4 with the same notations as Figure 3. The overall accuracy of PT predictions is similar to the equilateral case and we can notice, again, a significant improvement of one-loop predictions over tree-level ones.

As another example of the effects massive neutrinos have on the CDM bispectrum, in Fig. 5 we present the bispectrum for scalene triangles as a function of the angle θ between the two sides for all the cosmologies at $z = 0.5$ (left panel) and redshift $z = 1.0$ (right panel). We select triangle configurations in the mildly nonlinear regime, with $k_1 = 0.14 h \text{Mpc}^{-1}$, $k_2 = 0.23 h \text{Mpc}^{-1}$. The labels, colors and plots order correspond to those in figure 3. Differently from the previous cases, the bispectrum in massive neutrino cosmologies is suppressed on all scales shown. PT is able to reproduce the measurements in the different cosmologies quite well at $z = 1$ and large values of θ (the “squeezed limit”) while it shows the usual overestimation, about 10-15%, for more equilateral triangles and lower redshift.

An additional way to assess the effect of massive neutrinos on the bispectrum and compare it to the effect on the power spectrum, is to compute the reduced bispectrum Q defined as

$$Q(k_1, k_2, k_3) = \frac{B(k_1, k_2, k_3)}{P(k_1)P(k_2) + P(k_1)P(k_3) + P(k_2)P(k_3)}. \quad (4.5)$$

This quantity, at tree-level in PT, does not depend on the initial amplitude of the linear fluctuations (or σ_8 in a Λ CDM cosmology), including the suppression due to neutrinos in linear theory, and it highlights the different level of nonlinearity in the bispectrum w.r.t. the power spectrum. In all the figures 3, 4 and 5 the bottom part shows the reduced bispectrum for the choosen configurations at $z = 0.5$ and 1. Again, top panels show measurements for Q compared with tree-level and one-loop predictions; middle panels show the residuals with respect to one-loop, while in the bottom panels we display the ratios between the reduced bispectrum measured for $m_\nu \neq 0$ with respect to Λ CDM. The errors are computed by propagating ΔB and ΔP errors neglecting the cross-correlation between P and B .

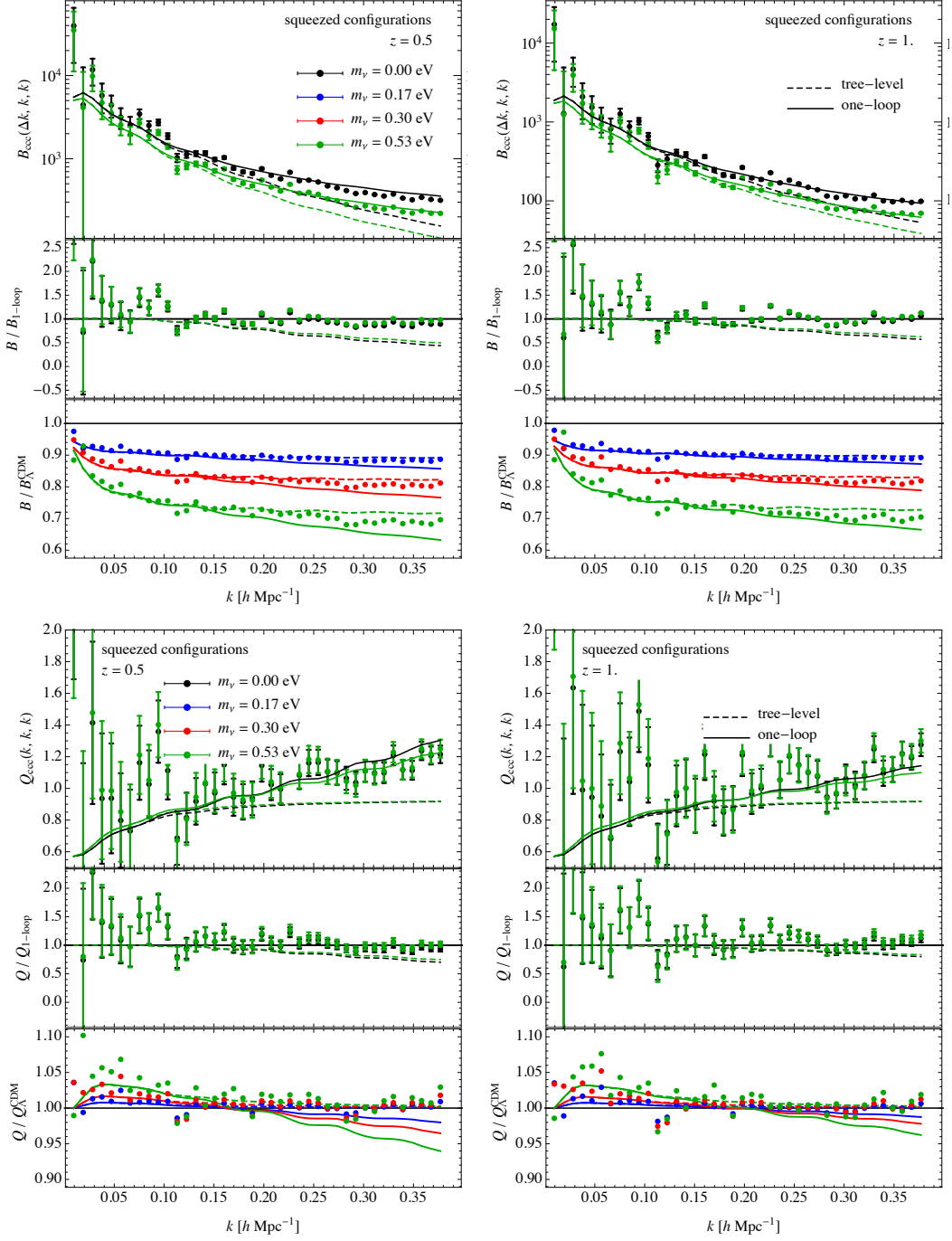


Figure 4. Same as figure 3 but for squeezed configurations $B_{ccc}(k_l, k, k)$ with fixed $k_l = 0.009 h \text{ Mpc}^{-1}$ as a function of k .

The small deviations we see in the bottom panels among different cosmologies indicate that any new, nonlinear neutrinos signature specific for the bispectrum is significantly small at scales $k > 0.2 h \text{ Mpc}^{-1}$. This implies that the bispectrum alone is not able to probe new physical effects induced by massive neutrinos in the clustering of dark matter; however it still represents a relevant

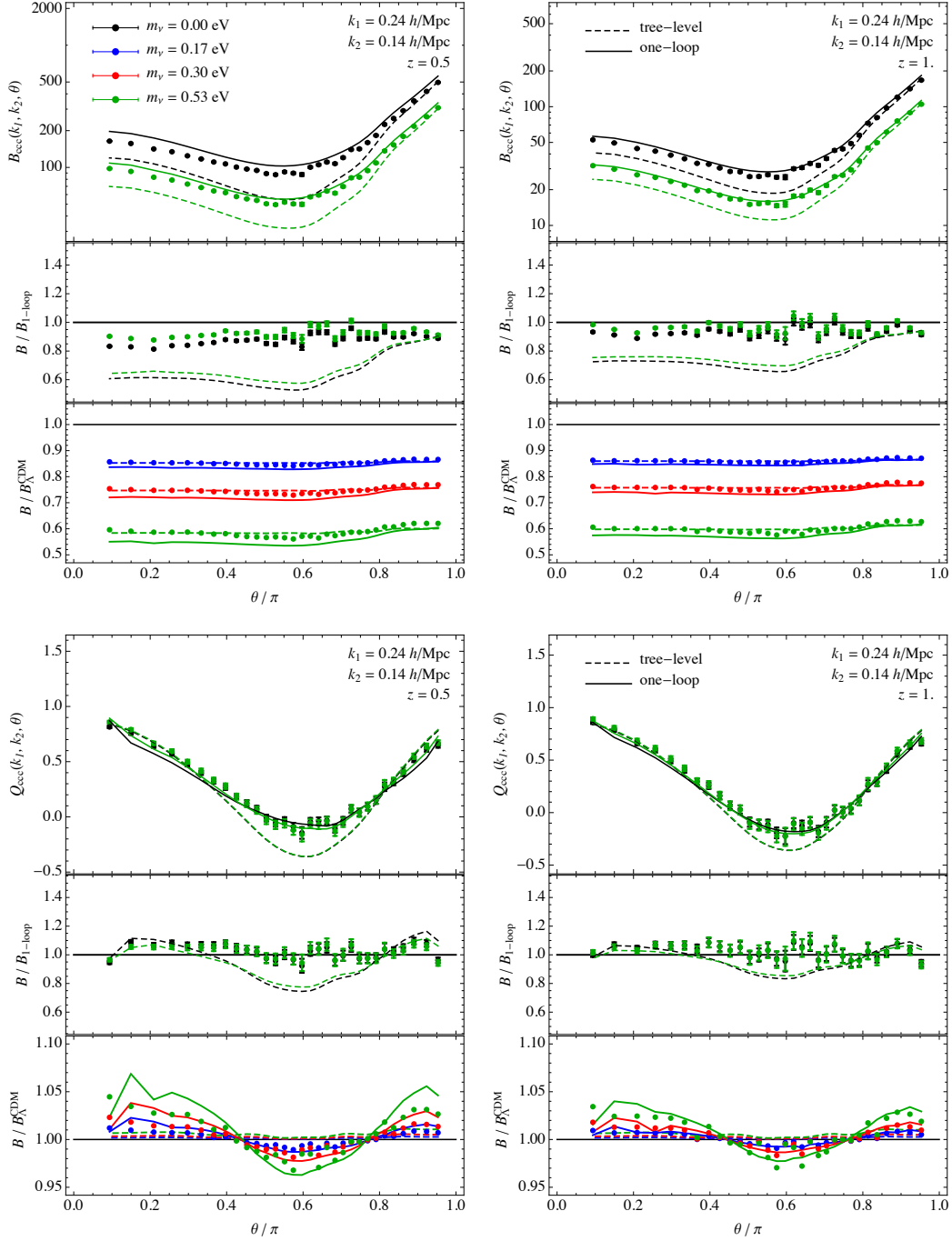


Figure 5. Same as figure 3 but for scalene configurations with fixed sides $k_1 = 0.14 h \text{ Mpc}^{-1}$ and $k_2 = 0.23 h \text{ Mpc}^{-1}$ as a function of the angle between \mathbf{k}_1 and \mathbf{k}_2 .

asset as it breaks part of the degeneracy between the cosmological parameters, when combined with the power spectrum. One-loop predictions for Q are well within the precision of our measurements. They are also qualitatively consistent with results for the relative effect of neutrino masses shown in the bottom panels, with the exception of the squeezed configurations at small scales where they

overpredict significantly a neutrino signature not detectable in the measurements. These are, however, few percent effects, too small to be properly investigated with the limited statistic of a single set of simulations.

5 The halo bispectrum

5.1 Bias modeling

According to the Eulerian bias model, at large scales, the halo density field δ_h can be locally described as a function of the underlying smoothed density contrast δ , [16, 66, 82]. In particular if $\delta \ll 1$, we can model δ_h as a Taylor expansion in δ ,

$$\delta_h = \sum_n \frac{b_n}{n!} \delta^n, \quad (5.1)$$

where the b_n correspond to the bias parameters. In this framework, the halo power spectrum, P_{hh} or the halo-matter cross correlation, at very large scales, are related to the matter power spectrum $P(k)$, through

$$P_{hh}(k) = b_1^2 P(k) \quad P_{hm} = b_1 P(k) \quad (5.2)$$

In a local Eulerian bias model the tree-level halo bispectrum reads

$$B_{hhh}(k_1, k_2, k_3) = b_1^3 B(k_1, k_2, k_3) + b_2 b_1^2 \Sigma_{123}(k_1, k_2, k_3), \quad (5.3)$$

with B being the matter bispectrum, $\Sigma_{123} \equiv P(k_1)P(k_2) + 2 \text{ cyc}$ and b_2 a quadratic bias parameter. The equation above shows that a measurements of the halo bispectrum on large scale could be used not only to constrain cosmological parameters, but also to break the degeneracy between the bias parameters and the amplitude of fluctuations in a power spectrum analysis.

It is well known, see *e.g.* [75, 83], that fitting B_{hhh} with model in eq. 5.3 yields different values of b_1 with respect to ones obtained from the halo power spectrum, modeled as in eq. 5.2. Recent works on bias modelling [54, 55, 84] have shown the intrinsic mistake in considering the bias to be deterministic and local: the nonlinear evolution induced by gravity introduces new, non-local bias contributions proportional to operators built from derivatives of the density field and/or the gravitational potential. In this framework the halo density, at second order in the bias expansion, takes the form

$$\delta_h = b_1 \delta + \frac{b_2}{2} \delta^2 + \gamma_2 \mathcal{G}_2, \quad (5.4)$$

where \mathcal{G}_2 is defined as

$$\mathcal{G}_2 \equiv (\nabla_{ij} \Phi_v)^2 - (\nabla_{ij} \Phi_v)^2, \quad (5.5)$$

with Φ_v being the velocity potential such that $\mathbf{v} = \nabla \Phi_v$. The resulting tree-level halo bispectrum reads

$$B_{hhh}(k_1, k_2, k_3) = b_1^3 B(k_1, k_2, k_3) + b_2 b_1^2 \Sigma_{123}(k_1, k_2, k_3) + 2\gamma_2 b_1^2 K_{123}(k_1, k_2, k_3), \quad (5.6)$$

where $K_{123} \equiv (\mu_{12} - 1)P(k_1)P(k_2) + 2 \text{ cyc}$, μ_{12} the cosine of the angle between \mathbf{k}_1 and \mathbf{k}_2 .

This model has been widely tested in Λ CDM cosmologies, and in this section we would like to extend these results to a cosmological model that include massive neutrinos. As first noted in [42], the linear bias in a cosmology with massive neutrinos is scale independent only if the CDM power spectrum appears on the right hand side of 5.2. This is a consequence of the fact that neutrinos do not cluster on halos or galaxies scales, and therefore fluctuations in the number of halos and galaxies respond to the CDM field only.

Given this result, we will model the halo bispectrum and then fit for the bias parameters in the next section assuming the halo bias relation in 5.4 is written in terms of the CDM field only. Recovering the same linear bias of the power spectrum from the bispectrum would yield a confirmation of the correctness of the argument for linear bias in [42].

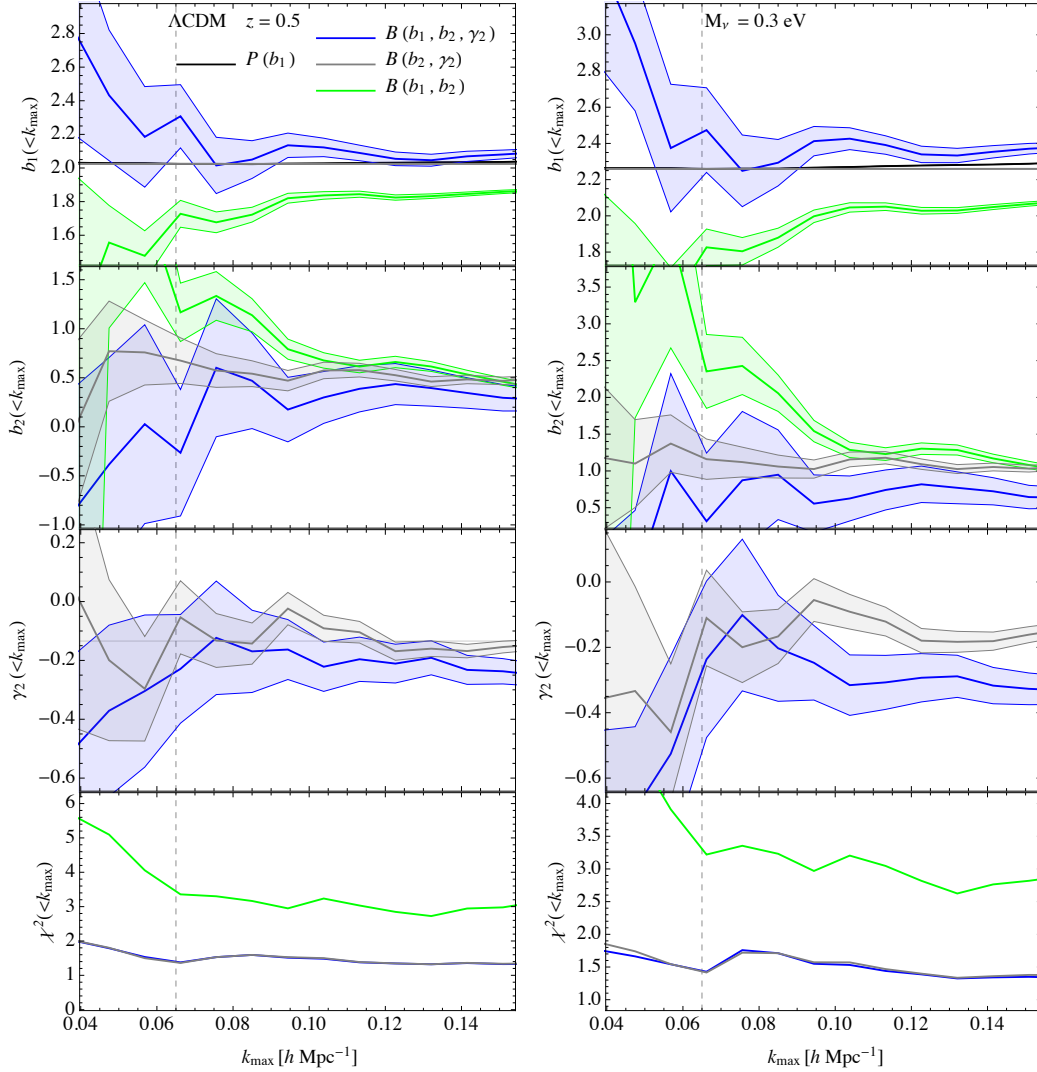


Figure 6. The best fits bias parameters in Λ CDM framework (left panel) and neutrino cosmologies $m_\nu = 0.53$ eV, (right panel), assuming a local and non local bias model, at $z = 0.5$. Green lines indicate the measurements of b_1 b_2 for the local model, (top and middle-top panels). Blue color indicates b_1 , the *effective* b_2 and the non local correction γ_2 (middle-bottom panels) to the bias model. Black lines correspond b_1 as measured from the halo power spectrum P_{hh} . Grey color shows the best fits for b_2 and γ_2 fixing b_1 from the power spectrum fits. In the bottom panels we show the χ^2 related to the different fitting formulas.

5.2 Fitting procedure

We measure the halo bispectrum in a Λ CDM cosmology and in cosmologies with all the three different values of neutrino masses, $m_\nu = 0.17, 0.3, 0.53$ eV. We do not consider a part of the measurements for the high-mass threshold, $M > 10^{14} M_\odot/h$, and redshift $z = 1.0$ since they are highly affected by shot-noise contributions, which for the halo bispectrum take the following form

$$\hat{B}_{hhh}(k_1, k_2, k_3) = B_{hhh}(k_1, k_2, k_3) + \frac{1}{\bar{n}} [P_{hh}(k_1) + 2 \text{cyc}] + \frac{1}{\bar{n}^2} \quad (5.7)$$

We compare the best fit measurements of b_1 and b_2 assuming a local model for the bias the values for b_1 , b_2 and γ_2 when assuming the non local model. At the level of two-point statistics we fit a

linear model to the halo-matter cross-correlation, $P_{hm}(k)$, as a function of the maximum wavenumber k_{max} . For the bispectrum we compute the likelihood \mathcal{L} up to a value k_{max} for the largest side for each triangle configuration. In the case of the non local model we have,

$$\ln \mathcal{L} = \sum_k^{k_{max}} \frac{B_{hhh} - b_1^3 B_c - b_2 b_1^2 \Sigma_{123} - 2\gamma_2 b_1^2 K_{123} - \alpha_1 (k_1^2 + k_2^2) (P_1 P_2) + 2 \text{cyc}}{\Delta B_{hhh}^2}, \quad (5.8)$$

with ΔB_{hhh}^2 as Eq. (4.3). A similar expression is used to estimate the linear bias from the halo-matter cross power spectrum, for which we also assume Gaussian covariance. Possible, unaccounted scale-dependences in the modeling are marginalized over the amplitude α of a generic k^2 -like term in both the likelihood for the power spectrum and the bispectrum. This term will take care of higher loop corrections and scale dependent bias on large scales [85, 86]. All the fits have been computed using the downhill simplex method, see *e.g.* [87]. We determined the errors on the best-fit values using the Fisher matrix prescription, see for instance [88]. In order to compare the results for b_2 from local *vs* non local models, we introduce an effective local quadratic bias, $b_{2,\text{eff}} = b_2 - 4/3\gamma_2$, [89], in case of the non local prescription, corresponding to the amplitude of the monopole component of the overall quadratic bias correction. For simplicity of notation, since we do not make use of the quadratic bias in the case of non local prescription, we will refer to $b_{2,\text{eff}}$ as b_2 , omitting the second subscript. The CDM bispectrum in the above equation is computed at 1-loop in perturbation theory, whereas the other terms are evaluated at tree-level, so we expect any failure of the theoretical predictions at low scales to be mainly due to the bias model.

In figure 6 we present the best fits of the bias parameters from the measurements in two different cosmologies, Λ CDM (left panels) and with $M_\nu = 0.3$ eV (right panels). Both figures are organised in the same way: the measurements of b_1 and b_2 at $z = 0.0$ (left panel) and at $z = 0.5$ (right panel); cyan and orange colours indicate b_1 and b_2 for the local model while blue and red colours indicate b_1 and *effective* b_2 for the non local prescription. Black lines correspond to the measurement of b_1 obtained from the halo-matter power spectrum P_{hm} . We noticed that the measurements of b_1 in a local bias framework disagree with the estimates from two-point statistics, but that on the other hand when we account for γ_2 , we find a good accordance; this confirms the effect of non-local bias on the halo bispectrum measurements even in a massive neutrino cosmology. It also reinforces our understanding of halo/galaxy bias in these cosmologies in terms of the CDM field only.

Even though the error budget of our measurements of the Bispectrum in the simulations does not allow us to test the bias model of the Bispectrum at the % level, it is still interesting to check down to which scale our bias model provides a reasonable fit to the bispectrum in the N-body. On the baryonic acoustic oscillations scales our errors are indeed comparable with those in the real data from [58]. Figure 7 shows the measurements of the bispectrum for equilateral and squeezed configurations. We selected the halo mass range A at redshifts $z = 0.5$. The dashed lines show the theoretical predictions for the matter bispectrum in case of Λ CDM (black) and cosmology with $M_\nu = 0.53$ eV (green). The continuous lines indicate the predictions for the halo bispectrum assuming a non local eulerian model for the bias. The agreement of the model with the data breaks down earlier in the presence of massive neutrinos, as the bias parameters are higher and therefore nonlinearities stronger. Nevertheless we find our bias template is able to fit the measured halo bispectrum down to $k \simeq 0.15 h \text{Mpc}^{-1}$. It is important also to notice that in comparison with the Λ CDM case the suppression in the halo bispectrum is more or less constant across the range of scale where PT gives a good fit to the measurements., revealing that difference in the shape of the underlying dark matter power spectrum are very degenerate with the bias parameters.

5.3 The universality of the halo bias at quadratic order

In the context of bias modeling, universality means that the bias coefficients, as a function of mass, cosmology and redshift, can be written in terms of the peak height $\nu \equiv \delta_{cr}/\sigma(M, z)$, defined as the ratio between the constant critical density $\delta_{cr} = 1.686$ for spherical collapse, and $\sigma(M, z)$, the r.m.s of the linear density field smoothed at a mass scale M and redshift z . Any dependence on the cosmological model, or redshift, is encoded in the function $\sigma(M, z)$. This is a very strong statement,

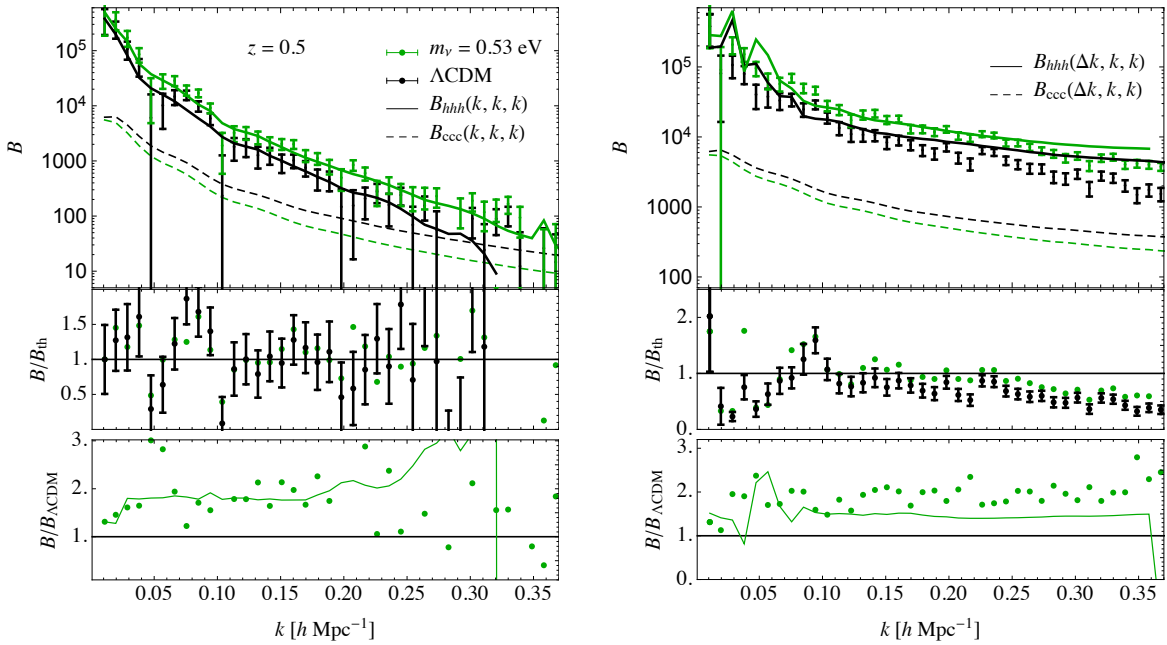


Figure 7. The measurements of the Bispectrum for equilateral and squeezed configurations. Dashed lines show the theoretical predictions for matter bispectrum in Λ CDM (black) and in cosmology with $M_\nu = 0.53eV$ (green). Continuous lines indicate the predictions for the halo bispectrum assuming a non local bias model; black and green points mark the measurements of the halo bispectrum at $M > 10^{13}M_\odot$.

and in principle of great value for cosmological analyses, as it allows to predict, for instance, the evolution of the bias parameters with redshift. Measurements in the N-body simulations of Λ CDM cosmologies show that bias parameters are universal functions of redshift [90–94].

In [42] it was shown that the same result applies to linear bias in massive neutrinos cosmologies if the peak height is computed from the variance of the CDM field, $\nu_c = \delta_{cr}/\sigma_c$. An incorrect choice for the variance leads to strong violations of universality with both redshift and cosmology. This is just a consequence of the fact that the proper bias expansion is written in terms of the CDM field. Given our measurements of the bispectrum and the best fit values of the bias coefficients, we are in the position to test universality beyond linear bias. Such an analysis is presented in Fig. 8. The top panel shows the best fit value for linear bias from the power spectrum as a function of ν_c . Different symbols and colors refer to different halo populations in different cosmologies, redshifts and mass thresholds. The figure agrees with [42] in showing $b_1(\nu_c)$ as a universal prediction, function of ν_c alone. The middle and bottom panel, in addition, show the universality of quadratic bias coefficients, both local and non local ones. We find that b_2 and γ_2 are universal functions of cosmology and redshift if the right variable, ν_c , is used. This is non-trivial check of the bias model and confirms our understanding of the clustering of halos in cosmologies with massive neutrinos. An important consequence of universality is the existence of smooth relations between linear bias and other bias parameters. Such relations, if calibrated with enough accuracy, can be used to reduce the number of nuisance parameters in a cosmological analysis. In particular the Eulerian bias model assumes that non local terms are only generated by gravitational evolution, yielding [55, 89],

$$\gamma_2 = -\frac{2}{7}(b_1 - 1), \quad (5.9)$$

which is assumed to be valid in all cosmological analysis of galaxy survey data [58, 95–97]. Recently [84, 94, 98, 99] have shown, in analytical calculations and measurements in N-body simulations of Λ CDM cosmologies, that, as a results of the fact that halo formation happens in a ellipsoidal fashion,

the above equation needs to be modified to include a Lagrangian non local coefficient γ_2^L ,

$$\gamma_2 = \gamma_2^L - \frac{2}{7}(b_1 - 1). \quad (5.10)$$

As a final application of our results on the halo bispectrum we therefore test the relations between bias parameters in cosmologies with massive neutrinos. In figure 8, we show b_2 , top panel, and γ_2 , bottom panel, as a function of linear bias. As expected, quadratic density bias is a smooth function of b_1 independently of the value of the neutrino masses. This implies that existing fitting formulae for $b_2(b_1)$ as in [93, 100] can be used in cosmologies with massive neutrinos. Moving to non local bias, we find that the prediction of Eq. 5.9 compare reasonably well with the measurements. For high values of ν where we expect bigger deviations from Eq. 5.9 our best fit values are too noisy to say anything conclusive. We plan to return to this issue in future work, as assumptions on non local bias can affect galaxy clustering analyses that use Lagrangian [101–103] or Eulerian [57, 58, 95, 96] perturbation theory.

6 Conclusions

In this work we have presented the first analysis of the matter and halo bispectrum from simulations of cosmologies with massive neutrinos described as a additional set of particles. We have measured the CDM and CDM+ ν bispectrum, which we have then compared to perturbation theory predictions. Firstly we have shown, using analytical arguments, that numerical approaches including neutrinos only at linear level or through response functions could potentially predict biased bispectra on large scales. From measurements in N-body simulations we showed that the CDM bispectrum, B_{ccc} is the dominant three-point statistics, with bispectra involving one or more neutrino fields being highly suppressed. This simplifies a lot the analytical evaluation, since only B_{ccc} needs to be computed beyond the tree level prediction. The perturbative calculations agrees fairly well with the N-body, most importantly at the same level it does in a standard cosmological simulation. We have shown that tree-level perturbation theory is sufficient to describe any bispectra involving one or more neutrino field, as their perturbations are highly suppressed below the free-streaming scale. We have also estimated non-linear neutrinos signatures in the bispectrum by looking at the reduce bispectrum, finding $< 1\%$ effects for the considerably high value of the neutrino masses considered in this paper.

We then devoted our attention to the halo bispectrum in cosmologies with massive neutrinos, the main motivation being the result in [42] that linear halo bias should be written in terms of the CDM field only. We extend this finding to higher order bias coefficients, showing that the halo bispectrum can be characterized by the same bias expansion is usually performed in a Λ CDM universe. This has important consequences for universality of higher order bias parameters, which holds if written in terms of the peak height of the CDM field, $\nu_c = \delta_{cr}/\sigma_c$. This implies, for instance, that quadratic bias, b_2 , can be written in terms of b_1 regardless of the value of neutrino masses.

Acknowledgments

The DEMNUni simulations were carried out at the Tier-0 IBM BG/Q machine, Fermi, of the Centro Interuniversitario del Nord-Est per il Calcolo Elettronico (CINECA, Bologna, Italy), via the five million cpu-hrs budget provided by the Italian SuperComputing Resource Allocation (ISCR) to the class-A proposal entitled “The Dark Energy and Massive-Neutrino Universe”. RR acknowledge support from the European Research Council through the Darksurvey grant 614030. CC acknowledges financial support from the European Research Council through the Darklight Advanced Research Grant (n. 291521), and the grant MIUR PRIN 2015 “Cosmology and Fundamental Physics: illuminating the Dark Universe with Euclid”. EC and ES would like to thank Francisco Villaescusa-Navarro, Matteo Viel and Julien Bel for useful discussions.

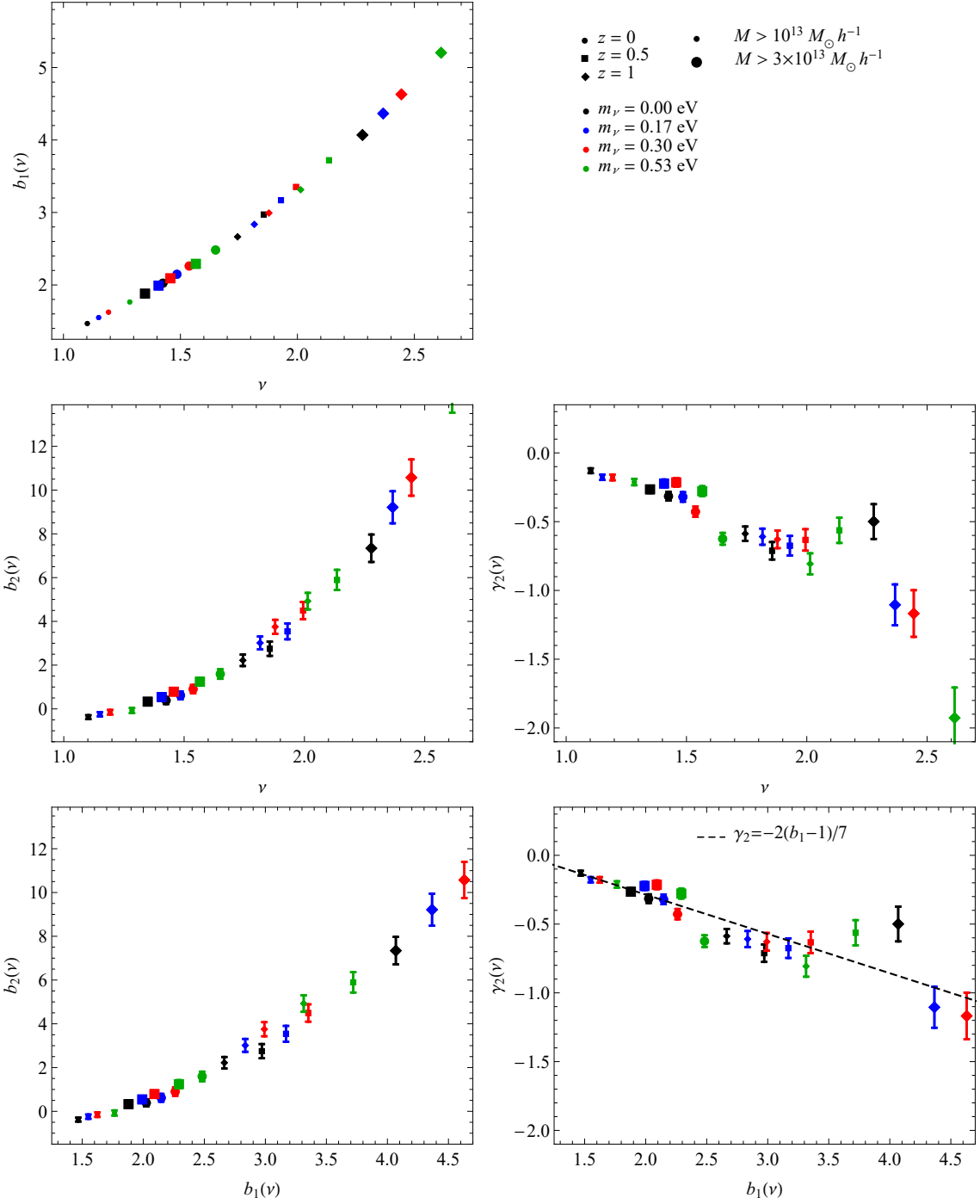


Figure 8. Upper panels: Best fit value for the bias parameters as a function the peak height for different cosmologies, redshift and halo mass threshold. Lower panels: Relation between second order bias parameter and linear bias for the same cosmological models, redshift and halo masses.

References

- [1] Planck Collaboration, P. A. R. Ade, N. Aghanim, M. Arnaud, M. Ashdown, J. Aumont et al., *Planck*

- 2015 results. XIII. Cosmological parameters, *Astron. Astrophys.* **594** (Sept., 2016) A13, [[1502.01589](#)].
- [2] S. Alam, M. Ata, S. Bailey, F. Beutler, D. Bizyaev, J. A. Blazek et al., *The clustering of galaxies in the completed SDSS-III Baryon Oscillation Spectroscopic Survey: cosmological analysis of the DR12 galaxy sample*, *ArXiv e-prints* (July, 2016) , [[1607.03155](#)].
- [3] G.-B. Zhao, M. Raveri, L. Pogosian, Y. Wang, R. G. Crittenden, W. J. Handley et al., *The clustering of galaxies in the completed SDSS-III Baryon Oscillation Spectroscopic Survey: Examining the observational evidence for dynamical dark energy*, *ArXiv e-prints* (Jan., 2017) , [[1701.08165](#)].
- [4] R. Laureijs, J. Amiaux, S. Arduini, J. . Auguères, J. Brinchmann, R. Cole et al., *Euclid Definition Study Report*, *ArXiv: 1110.3193* (Oct., 2011) , [[1110.3193](#)].
- [5] M. Levi, C. Bebek, T. Beers, R. Blum, R. Cahn, D. Eisenstein et al., *The DESI Experiment, a whitepaper for Snowmass 2013*, *ArXiv: 1308.0847* (Aug., 2013) , [[1308.0847](#)].
- [6] LSST Science Collaboration, P. Marshall, T. Anguita, F. B. Bianco, E. C. Bellm, N. Brandt et al., *Science-Driven Optimization of the LSST Observing Strategy*, *ArXiv e-prints* (Aug., 2017) , [[1708.04058](#)].
- [7] P. McDonald and D. J. Eisenstein, *Dark energy and curvature from a future baryonic acoustic oscillation survey using the Lyman- α forest*, *Phys. Rev. D* **76** (Sept., 2007) 063009, [[astro-ph/0607122](#)].
- [8] D. J. Eisenstein, H.-J. Seo and M. White, *On the Robustness of the Acoustic Scale in the Low-Redshift Clustering of Matter*, *Astrophys. J.* **664** (Aug., 2007) 660–674, [[astro-ph/0604361](#)].
- [9] C. Carbone, A. Mangilli and L. Verde, *Isocurvature modes and Baryon Acoustic Oscillations II: gains from combining CMB and Large Scale Structure*, *Journal of Cosmology and Astro-Particle Physics* **9** (Sept., 2011) 028, [[1107.1211](#)].
- [10] E. Giusarma, M. Corsi, M. Archidiacono, R. de Putter, A. Melchiorri, O. Mena et al., *Constraints on massive sterile neutrino species from current and future cosmological data*, *Phys. Rev. D* **83** (June, 2011) 115023, [[1102.4774](#)].
- [11] L. Amendola, S. Appleby, D. Bacon, T. Baker, M. Baldi, N. Bartolo et al., *Cosmology and Fundamental Physics with the Euclid Satellite*, *Living Reviews in Relativity* **16** (Sept., 2013) , [[1206.1225](#)].
- [12] D. H. Weinberg, M. J. Mortonson, D. J. Eisenstein, C. Hirata, A. G. Riess and E. Rozo, *Observational probes of cosmic acceleration*, *Phys. Rep.* **530** (Sept., 2013) 87–255, [[1201.2434](#)].
- [13] B. Audren, J. Lesgourgues, S. Bird, M. G. Haehnelt and M. Viel, *Neutrino masses and cosmological parameters from a Euclid-like survey: Markov Chain Monte Carlo forecasts including theoretical errors*, *Journal of Cosmology and Astro-Particle Physics* **1** (Jan., 2013) 26, [[1210.2194](#)].
- [14] A. Joyce, B. Jain, J. Khoury and M. Trodden, *Beyond the cosmological standard model*, *Phys. Rep.* **568** (Mar., 2015) 1–98, [[1407.0059](#)].
- [15] T. Baldauf, M. Mirbabayi, M. Simonović and M. Zaldarriaga, *LSS constraints with controlled theoretical uncertainties*, *ArXiv e-prints* (Feb., 2016) , [[1602.00674](#)].
- [16] V. Desjacques, D. Jeong and F. Schmidt, *Large-Scale Galaxy Bias*, *ArXiv e-prints* (Nov., 2016) , [[1611.09787](#)].
- [17] K. Koyama, *Cosmological tests of modified gravity*, *Reports on Progress in Physics* **79** (Apr., 2016) 046902, [[1504.04623](#)].
- [18] D. Alonso, E. Bellini, P. G. Ferreira and M. Zumalacárregui, *Observational future of cosmological scalar-tensor theories*, *Phys. Rev. D* **95** (Mar., 2017) 063502, [[1610.09290](#)].
- [19] J. Lesgourgues and S. Pastor, *Massive neutrinos and cosmology*, *Phys. Rep.* **429** (July, 2006) 307–379, [[astro-ph/0603494](#)].
- [20] J. Lesgourgues, G. Mangano, G. Miele and S. Pastor, *Neutrino Cosmology*. Cambridge, UK: Cambridge University Press, Feb., 2013.

- [21] N. Palanque-Delabrouille, C. Yèche, J. Baur, C. Magneville, G. Rossi, J. Lesgourgues et al., *Neutrino masses and cosmology with Lyman-alpha forest power spectrum*, *Journal of Cosmology and Astro-Particle Physics* **11** (Nov., 2015) 011, [[1506.05976](#)].
- [22] Planck Collaboration, P. A. R. Ade, N. Aghanim, M. Arnaud, M. Ashdown, J. Aumont et al., *Planck 2015 results. XXIV. Cosmology from Sunyaev-Zeldovich cluster counts*, *Astron. Astrophys.* **594** (Sept., 2016) A24, [[1502.01597](#)].
- [23] A. J. Cuesta, V. Niro and L. Verde, *Neutrino mass limits: Robust information from the power spectrum of galaxy surveys*, *Physics of the Dark Universe* **13** (Sept., 2016) 77–86, [[1511.05983](#)].
- [24] S. Vagnozzi, E. Giusarma, O. Mena, K. Freese, M. Gerbino, S. Ho et al., *Unveiling ν secrets with cosmological data: neutrino masses and mass hierarchy*, *ArXiv e-prints* (Jan., 2017) , [[1701.08172](#)].
- [25] M. Archidiacono, T. Brinckmann, J. Lesgourgues and V. Poulin, *Physical effects involved in the measurements of neutrino masses with future cosmological data*, *Journal of Cosmology and Astro-Particle Physics* **2** (Feb., 2017) 052, [[1610.09852](#)].
- [26] S. Saito, M. Takada and A. Taruya, *Impact of Massive Neutrinos on the Nonlinear Matter Power Spectrum*, *Physical Review Letters* **100** (May, 2008) 191301, [[0801.0607](#)].
- [27] Y. Y. Y. Wong, *Higher order corrections to the large scale matter power spectrum in the presence of massive neutrinos*, *Journal of Cosmology and Astro-Particle Physics* **10** (Oct., 2008) 35, [[0809.0693](#)].
- [28] J. Lesgourgues, S. Matarrese, M. Pietroni and A. Riotto, *Non-linear power spectrum including massive neutrinos: the time-rq flow approach*, *Journal of Cosmology and Astro-Particle Physics* **6** (June, 2009) 17, [[arXiv: 0901.4550 \[astro-ph.CO\]](#)].
- [29] A. Upadhye, R. Biswas, A. Pope, K. Heitmann, S. Habib, H. Finkel et al., *Large-scale structure formation with massive neutrinos and dynamical dark energy*, *Phys. Rev. D* **89** (May, 2014) 103515, [[1309.5872](#)].
- [30] D. Blas, M. Garny, T. Konstandin and J. Lesgourgues, *Structure formation with massive neutrinos: going beyond linear theory*, *Journal of Cosmology and Astro-Particle Physics* **11** (Nov., 2014) 039, [[1408.2995](#)].
- [31] H. Dupuy and F. Bernardeau, *Describing massive neutrinos in cosmology as a collection of independent flows*, *Journal of Cosmology and Astro-Particle Physics* **1** (Jan., 2014) 30, [[1311.5487](#)].
- [32] H. Dupuy and F. Bernardeau, *On the importance of nonlinear couplings in large-scale neutrino streams*, *Journal of Cosmology and Astro-Particle Physics* **8** (Aug., 2015) 053, [[1503.05707](#)].
- [33] E. Castorina, C. Carbone, J. Bel, E. Sefusatti and K. Dolag, *DEMNUi: the clustering of large-scale structures in the presence of massive neutrinos*, *Journal of Cosmology and Astro-Particle Physics* **7** (July, 2015) 043, [[1505.07148](#)].
- [34] F. Führer and Y. Y. Y. Wong, *Higher-order massive neutrino perturbations in large-scale structure*, *Journal of Cosmology and Astro-Particle Physics* **3** (Mar., 2015) 046, [[1412.2764](#)].
- [35] A. Upadhye, J. Kwan, A. Pope, K. Heitmann, S. Habib, H. Finkel et al., *Redshift-space distortions in massive neutrino and evolving dark energy cosmologies*, *Phys. Rev. D* **93** (Mar., 2016) 063515, [[1506.07526](#)].
- [36] M. Archidiacono and S. Hannestad, *Efficient calculation of cosmological neutrino clustering in the non-linear regime*, *Journal of Cosmology and Astro-Particle Physics* **6** (June, 2016) 018, [[1510.02907](#)].
- [37] M. Levi and Z. Vlah, *Massive neutrinos in nonlinear large scale structure: A consistent perturbation theory*, *ArXiv e-prints* (May, 2016) , [[1605.09417](#)].
- [38] J. Liu, S. Bird, J. M. Zorrilla Matilla, J. C. Hill, Z. Haiman, M. S. Madhavacheril et al., *MassiveNuS: Cosmological Massive Neutrino Simulations*, *ArXiv e-prints* (Nov., 2017) , [[1711.10524](#)].
- [39] F. Villaescusa-Navarro, F. Marulli, M. Viel, E. Branchini, E. Castorina, E. Sefusatti et al., *Cosmology with massive neutrinos I: towards a realistic modeling of the relation between matter, haloes and galaxies*, *Journal of Cosmology and Astro-Particle Physics* **3** (Mar., 2014) 11, [[1311.0866](#)].
- [40] Y. Liu, Y. Liang, H.-R. Yu, C. Zhao, J. Qin and T.-J. Zhang, *Baryon Acoustic Oscillation detections from the clustering of massive halos and different density region tracers in TianNu simulation*, *ArXiv e-prints* (Dec., 2017) , [[1712.01002](#)].

- [41] K. Ichiki and M. Takada, *Impact of massive neutrinos on the abundance of massive clusters*, *Phys. Rev. D* **85** (Mar., 2012) 063521, [[1108.4688](#)].
- [42] E. Castorina, E. Sefusatti, R. K. Sheth, F. Villaescusa-Navarro and M. Viel, *Cosmology with massive neutrinos II: on the universality of the halo mass function and bias*, *Journal of Cosmology and Astro-Particle Physics* **2** (Feb., 2014) 49, [[1311.1212](#)].
- [43] M. Costanzi, F. Villaescusa-Navarro, M. Viel, J.-Q. Xia, S. Borgani, E. Castorina et al., *Cosmology with massive neutrinos III: the halo mass function and an application to galaxy clusters*, *Journal of Cosmology and Astro-Particle Physics* **12** (Dec., 2013) 12, [[1311.1514](#)].
- [44] M. LoVerde, *Spherical collapse in $\nu\Lambda$ CDM*, *Phys. Rev. D* **90** (Oct., 2014) 083518, [[1405.4858](#)].
- [45] M. Biagetti, K. C. Chan, V. Desjacques and A. Paranjape, *Measuring non-local Lagrangian peak bias*, *Mon. Not. R. Astron. Soc.* **441** (June, 2014) 1457–1467, [[1310.1401](#)].
- [46] M. LoVerde and M. Zaldarriaga, *Neutrino clustering around spherical dark matter halos*, *Phys. Rev. D* **89** (Mar., 2014) 063502, [[1310.6459](#)].
- [47] M. LoVerde, *Neutrino mass without cosmic variance*, *Phys. Rev. D* **93** (May, 2016) 103526, [[1602.08108](#)].
- [48] C.-T. Chiang, W. Hu, Y. Li and M. LoVerde, *Scale-dependent bias and bispectrum in neutrino separate universe simulations*, *ArXiv e-prints* (Oct., 2017) , [[1710.01310](#)].
- [49] E. Massara, F. Villaescusa-Navarro, M. Viel and P. M. Sutter, *Voids in massive neutrino cosmologies*, *Journal of Cosmology and Astro-Particle Physics* **11** (Nov., 2015) 018, [[1506.03088](#)].
- [50] H.-M. Zhu, U.-L. Pen, X. Chen, D. Inman and Y. Yu, *Measurement of Neutrino Masses from Relative Velocities*, *Physical Review Letters* **113** (Sept., 2014) 131301, [[1311.3422](#)].
- [51] C. Okoli, M. I. Scrimgeour, N. Afshordi and M. J. Hudson, *Dynamical friction in the primordial neutrino sea*, *ArXiv e-prints* (Nov., 2016) , [[1611.04589](#)].
- [52] L. Senatore and M. Zaldarriaga, *The Effective Field Theory of Large-Scale Structure in the presence of Massive Neutrinos*, *ArXiv e-prints* (July, 2017) , [[1707.04698](#)].
- [53] M. Shoji and E. Komatsu, *Massive neutrinos in cosmology: Analytic solutions and fluid approximation*, *Phys. Rev. D* **81** (June, 2010) 123516.
- [54] K. C. Chan, R. Scoccimarro and R. K. Sheth, *Gravity and large-scale nonlocal bias*, *Phys. Rev. D* **85** (Apr., 2012) 083509, [[1201.3614](#)].
- [55] T. Baldauf, U. Seljak, V. Desjacques and P. McDonald, *Evidence for quadratic tidal tensor bias from the halo bispectrum*, *Phys. Rev. D* **86** (Oct., 2012) 083540, [[1201.4827](#)].
- [56] E. Sefusatti, M. Crocce, S. Pueblas and R. Scoccimarro, *Cosmology and the bispectrum*, *Phys. Rev. D* **74** (July, 2006) 023522, [[arXiv: astro-ph/0604505](#)].
- [57] Z. Slepian, D. J. Eisenstein, J. R. Brownstein, C.-H. Chuang, H. Gil-Marín, S. Ho et al., *Detection of Baryon Acoustic Oscillation Features in the Large-Scale 3-Point Correlation Function of SDSS BOSS DR12 CMASS Galaxies*, *ArXiv e-prints* (July, 2016) , [[1607.06097](#)].
- [58] H. Gil-Marín, W. J. Percival, L. Verde, J. R. Brownstein, C.-H. Chuang, F.-S. Kitaura et al., *The clustering of galaxies in the SDSS-III Baryon Oscillation Spectroscopic Survey: RSD measurement from the power spectrum and bispectrum of the DR12 BOSS galaxies*, *Mon. Not. R. Astron. Soc.* **465** (Feb., 2017) 1757–1788, [[1606.00439](#)].
- [59] W. Hu, D. J. Eisenstein and M. Tegmark, *Weighing Neutrinos with Galaxy Surveys*, *Physical Review Letters* **80** (June, 1998) 5255–5258, [[astro-ph/9712057](#)].
- [60] J. Brandbyge, S. Hannestad, T. Haugbølle and B. Thomsen, *The effect of thermal neutrino motion on the non-linear cosmological matter power spectrum*, *Journal of Cosmology and Astro-Particle Physics* **8** (Aug., 2008) 020, [[0802.3700](#)].
- [61] M. Viel, M. G. Haehnelt and V. Springel, *The effect of neutrinos on the matter distribution as probed by the intergalactic medium*, *Journal of Cosmology and Astro-Particle Physics* **6** (June, 2010) 15, [[1003.2422](#)].

- [62] S. Bird, M. Viel and M. G. Haehnelt, *Massive neutrinos and the non-linear matter power spectrum*, *Mon. Not. R. Astron. Soc.* **420** (Mar., 2012) 2551–2561, [[1109.4416](#)].
- [63] C. Wagner, L. Verde and R. Jimenez, *Effects of the Neutrino Mass Splitting on the Nonlinear Matter Power Spectrum*, *Astrophys. J. Lett.* **752** (June, 2012) L31, [[1203.5342](#)].
- [64] D. Inman, J. D. Emberson, U.-L. Pen, A. Farchi, H.-R. Yu and J. Harnois-Déraps, *Precision reconstruction of the cold dark matter-neutrino relative velocity from N -body simulations*, *Phys. Rev. D* **92** (July, 2015) 023502, [[1503.07480](#)].
- [65] H.-R. Yu, J. D. Emberson, D. Inman, T.-J. Zhang, U.-L. Pen, J. Harnois-Déraps et al., *Differential neutrino condensation onto cosmic structure*, *Nature Astronomy* **1** (July, 2017) 0143, [[1609.08968](#)].
- [66] F. Bernardeau, S. Colombi, E. Gaztañaga and R. Scoccimarro, *Large-scale structure of the universe and cosmological perturbation theory*, *Phys. Rep.* **367** (Sept., 2002) 1–3, [[astro-ph/0112551](#)].
- [67] C. Carbone, M. Petkova and K. Dolag, *DEMUNi: ISW, Rees-Sciama, and weak-lensing in the presence of massive neutrinos*, *Journal of Cosmology and Astro-Particle Physics* **7** (July, 2016) 034, [[1605.02024](#)].
- [68] Planck Collaboration, P. A. R. Ade, N. Aghanim, C. Armitage-Caplan, M. Arnaud, M. Ashdown et al., *Planck 2013 results. XVI. Cosmological parameters*, *Astron. Astrophys.* **571** (Nov., 2014) A16, [[1303.5076](#)].
- [69] V. Springel, S. D. M. White, A. Jenkins, C. S. Frenk, N. Yoshida, L. Gao et al., *Simulations of the formation, evolution and clustering of galaxies and quasars*, *Nature* **435** (June, 2005) 629–636, [[arXiv:astro-ph/0504097](#)].
- [70] V. Springel, N. Yoshida and S. D. M. White, *GADGET: a code for collisionless and gasdynamical cosmological simulations*, *New Astronomy* **6** (Apr., 2001) 79–117, [[astro-ph/0003162](#)].
- [71] K. Dolag, S. Borgani, G. Murante and V. Springel, *Substructures in hydrodynamical cluster simulations*, *Mon. Not. R. Astron. Soc.* **399** (Oct., 2009) 497–514, [[0808.3401](#)].
- [72] M. Davis, G. P. Efstathiou, C. S. Frenk and S. D. M. White, *The evolution of large-scale structure in a universe dominated by cold dark matter*, *Astrophys. J.* **292** (May, 1985) 371–394.
- [73] R. Scoccimarro, *Fast estimators for redshift-space clustering*, *Phys. Rev. D* **92** (Oct., 2015) 083532, [[1506.02729](#)].
- [74] E. Sefusatti, M. Crocce, R. Scoccimarro and H. M. P. Couchman, *Accurate estimators of correlation functions in Fourier space*, *Mon. Not. R. Astron. Soc.* **460** (Aug., 2016) 3624–3636, [[1512.07295](#)].
- [75] R. Scoccimarro, *The bispectrum: From theory to observations*, *Astrophys. J.* **544** (Dec., 2000) 597–615, [[astro-ph/0004086](#)].
- [76] E. Sefusatti, *One-loop perturbative corrections to the matter and galaxy bispectrum with non-gaussian initial conditions*, *Phys. Rev. D* **80** (Dec., 2009) 123002, [[0905.0717](#)].
- [77] S. Saito, M. Takada and A. Taruya, *Nonlinear power spectrum in the presence of massive neutrinos: Perturbation theory approach, galaxy bias, and parameter forecasts*, *Phys. Rev. D* **80** (Oct., 2009) 083528, [[0907.2922](#)].
- [78] R. Scoccimarro, S. Colombi, J. N. Fry, J. A. Frieman, E. Hivon and A. Melott, *Nonlinear evolution of the bispectrum of cosmological perturbations*, *Astrophys. J.* **496** (Mar., 1998) 586, [[astro-ph/9704075](#)].
- [79] E. Sefusatti, M. Crocce and V. Desjacques, *The matter bispectrum in N -body simulations with non-Gaussian initial conditions*, *Mon. Not. R. Astron. Soc.* **406** (Aug., 2010) 1014–1028, [[1003.0007](#)].
- [80] J. J. M. Carrasco, M. P. Hertzberg and L. Senatore, *The effective field theory of cosmological large scale structures*, *Journal of High Energy Physics* **9** (Sept., 2012) 82, [[1206.2926](#)].
- [81] R. E. Angulo, S. Foreman, M. Schmittfull and L. Senatore, *The one-loop matter bispectrum in the Effective Field Theory of Large Scale Structures*, *Journal of Cosmology and Astro-Particle Physics* **10** (Oct., 2015) 039, [[1406.4143](#)].
- [82] J. N. Fry and E. Gaztañaga, *Biasing and hierarchical statistics in large-scale structure*, *Astrophys. J.* **413** (Aug., 1993) 447–452, [[astro-ph/9302009](#)].

- [83] J. E. Pollack, R. E. Smith and C. Porciani, *Modelling large-scale halo bias using the bispectrum*, *Mon. Not. R. Astron. Soc.* **420** (Mar., 2012) 3469–3489, [[1109.3458](#)].
- [84] R. K. Sheth, K. C. Chan and R. Scoccimarro, *Nonlocal Lagrangian bias*, *Phys. Rev. D* **87** (Apr., 2013) 083002, [[1207.7117](#)].
- [85] J. J. M. Carrasco, M. P. Hertzberg and L. Senatore, *The effective field theory of cosmological large scale structures*, *Journal of High Energy Physics* **9** (Sept., 2012) 82, [[1206.2926](#)].
- [86] V. Desjacques, M. Crocce, R. Scoccimarro and R. K. Sheth, *Modeling scale-dependent bias on the baryonic acoustic scale with the statistics of peaks of Gaussian random fields*, *Phys. Rev. D* **82** (Nov., 2010) 103529, [[1009.3449](#)].
- [87] W. H. Press, S. A. Teukolsky, W. T. Vetterling and B. P. Flannery, *Numerical recipes in FORTRAN. The art of scientific computing*. Cambridge: University Press, 1992.
- [88] M. Tegmark, A. N. Taylor and A. F. Heavens, *Karhunen-loeve eigenvalue problems in cosmology: How should we tackle large data sets?*, *Astrophys. J.* **480** (May, 1997) 22, [[arXiv:astro-ph/9603021](#)].
- [89] K. C. Chan and R. Scoccimarro, *Halo sampling, local bias, and loop corrections*, *Phys. Rev. D* **86** (Nov., 2012) 103519, [[1204.5770](#)].
- [90] R. K. Sheth and G. Tormen, *Large-scale bias and the peak background split*, *Mon. Not. R. Astron. Soc.* **308** (Sept., 1999) 119–126, [[astro-ph/9901122](#)].
- [91] J. L. Tinker, B. E. Robertson, A. V. Kravtsov, A. Klypin, M. S. Warren, G. Yepes et al., *The Large-scale Bias of Dark Matter Halos: Numerical Calibration and Model Tests*, *Astrophys. J.* **724** (Dec., 2010) 878–886, [[1001.3162](#)].
- [92] K. Hoffmann, J. Bel and E. Gaztañaga, *Comparing halo bias from abundance and clustering*, *ArXiv e-prints* (Mar., 2015) , [[1503.00313](#)].
- [93] T. Lazeyras, C. Wagner, T. Baldauf and F. Schmidt, *Precision measurement of the local bias of dark matter halos*, *Journal of Cosmology and Astro-Particle Physics* **2** (Feb., 2016) 018, [[1511.01096](#)].
- [94] C. Modi, E. Castorina and U. Seljak, *Halo bias in Lagrangian space: estimators and theoretical predictions*, *Mon. Not. R. Astron. Soc.* **472** (Dec., 2017) 3959–3970, [[1612.01621](#)].
- [95] A. G. Sánchez, R. Scoccimarro, M. Crocce, J. N. Grieb, S. Salazar-Albornoz, C. Dalla Vecchia et al., *The clustering of galaxies in the completed SDSS-III Baryon Oscillation Spectroscopic Survey: Cosmological implications of the configuration-space clustering wedges*, *Mon. Not. R. Astron. Soc.* **464** (Jan., 2017) 1640–1658, [[1607.03147](#)].
- [96] F. Beutler, H.-J. Seo, A. J. Ross, P. McDonald, S. Saito, A. S. Bolton et al., *The clustering of galaxies in the completed SDSS-III Baryon Oscillation Spectroscopic Survey: baryon acoustic oscillations in the Fourier space*, *Mon. Not. R. Astron. Soc.* **464** (Jan., 2017) 3409–3430, [[1607.03149](#)].
- [97] Z. Slepian and D. J. Eisenstein, *Modelling the large-scale redshift-space 3-point correlation function of galaxies*, *Mon. Not. R. Astron. Soc.* **469** (Aug., 2017) 2059–2076, [[1607.03109](#)].
- [98] E. Castorina, A. Paranjape, O. Hahn and R. K. Sheth, *Excursion set peaks: the role of shear*, *ArXiv e-prints* (Nov., 2016) , [[1611.03619](#)].
- [99] E. Castorina, A. Paranjape and R. K. Sheth, *Constraints on halo formation from cross-correlations with correlated variables*, *Mon. Not. R. Astron. Soc.* **468** (July, 2017) 3813–3827, [[1611.03613](#)].
- [100] K. Hoffmann, J. Bel and E. Gaztañaga, *Linear and non-linear bias: predictions versus measurements*, *Mon. Not. R. Astron. Soc.* **465** (Feb., 2017) 2225–2235, [[1607.01024](#)].
- [101] C.-H. Chuang, M. Pellejero-Ibanez, S. Rodríguez-Torres, A. J. Ross, G.-b. Zhao, Y. Wang et al., *The clustering of galaxies in the completed SDSS-III Baryon Oscillation Spectroscopic Survey: single-probe measurements from DR12 galaxy clustering - towards an accurate model*, *Mon. Not. R. Astron. Soc.* **471** (Oct., 2017) 2370–2390, [[1607.03151](#)].
- [102] L. Wang, B. Reid and M. White, *An analytic model for redshift-space distortions*, *Mon. Not. R. Astron. Soc.* **437** (Jan., 2014) 588–599, [[1306.1804](#)].
- [103] Z. Vlah, U. Seljak and T. Baldauf, *Lagrangian perturbation theory at one loop order: Successes, failures, and improvements*, *Phys. Rev. D* **91** (Jan., 2015) 023508, [[1410.1617](#)].